POLITECNICO DI TORINO
Repository ISTITUZIONALE

Assessment of the Feasibility of Breast Lesion Detection with Contrast Source Inversion for Microwave Tomography: A Virtual Experiment

Original
Assessment of the Feasibility of Breast Lesion Detection with Contrast Source Inversion for Microwave Tomography: A Virtual Experiment / Ronca, Alessandra; Arduino, Alessandro; Zilberti, Luca; Bottauscio, Oriano; Tiberi, Gianluigi. - ELETTRONICO. - (2024), pp. 1-5. (Intervento presentato al convegno 18th European Conference on Antennas and Propagation (EuCAP) tenutosi a Glasgow (United Kingdom) nel 17-23 marzo 2024) [10.23919/eucap60739.2024.10501105].

Availability:
This version is available at: 11583/2988262 since: 2024-05-13T07:38:48Z

Publisher:
IEEE

Published
DOI:10.23919/eucap60739.2024.10501105

Terms of use:

This article is made available under terms and conditions as specified in the corresponding bibliographic description in the repository

Publisher copyright
IEEE postprint/Author's Accepted Manuscript

©2024 IEEE. Personal use of this material is permitted. Permission from IEEE must be obtained for all other uses, in any current or future media, including reprinting/republishing this material for advertising or promotional purposes, creating new collecting works, for resale or lists, or reuse of any copyrighted component of this work in other works.

(Article begins on next page)

25 May 2024

Assessment of the Feasibility of Breast Lesion Detection with Contrast Source Inversion for Microwave Tomography: A Virtual Experiment

Alessandra Ronca[1,2], Alessandro Arduino[2], Luca Zilberti[2], Oriano Bottauscio[2], Gianluigi Tiberi[3,4]
[1] Politecnico di Torino, Torino, Italy, alessandra.ronca@polito.it
[2] Istituto Nazionale di Ricerca Metrologica (INRiM), Torino, Italy
[3] Umbria Bioengineering Technologies, UBT Srl, Perugia, Italy
4 School of Engineering, London South Bank University, London, UK

***Abstract*—In this paper, the microwave tomography performed using the contrast source inversion method was investigated. A two-dimensional model problem, composed of a cylindrical phantom positioned at the center of the receiving antennas' circular distribution, provided the setup for virtual experiments. Both a homogeneous phantom, with electrical properties that approximate the ones of a dense breast, and several heterogeneous phantoms, with an inclusion whose high electrical properties simulate those of a breast lesion, were considered. The effect of the initial guess on the reconstruction of the homogeneous phantom was assessed for a first investigation. Then, the detectability of the inclusion in the heterogeneous phantom was tested varying its size, position, and electrical properties. Results suggested that *a priori* information is useful to build a robust initial guess. The inclusion was detectable in the permittivity maps independently of the considered dimension and position, whereas structured noise was predominant in the conductivity maps.**

***Index Terms*—contrast source inversion, electrical properties, mammography, microwave tomography**

I. Introduction

Quantitative reconstruction of the electric properties (EPs) of samples via electromagnetic imaging techniques is of paramount significance for a variety of disciplines, including biomedical applications. Breast cancer diagnosis is one extensively explored area, taking advantage of the significant dielectric contrast between malignant and healthy tissues [1].

Nowadays, mammography is the gold standard technology for mammographic screening. However, it has some limitations and potential harms, such as the use of ionizing radiation, breast compression, and performance restrictions due to the intrinsic nature of X-rays. Besides, the results are highly affected by breast density. In general, women are eligible for biannual screening after the age of 49 to minimize the impact of ionizing radiation. Nevertheless, recent studies estimate that (worldwide) almost 30 % of breast cancer cases occur in women when they are younger than 50 years old [2].

In this scenario, systems based on non-ionizing radiation are esteemed for a wide screening, with neither age nor follow-up examination interval restrictions [3]. In the last years, the scientific community made many efforts to develop methods capable of measuring non-invasively the distribution of the EPs inside a human body at microwave frequencies [4]. Such efforts have been encouraged by the fact that, at microwave frequencies, some physiopathological statuses based on tissue EPs can be distinguished. As described in [5], the EPs in the range of microwaves (4 GHz – 8 GHz) differ greatly depending on the tissues. For electrical permittivity, the value of a benign tumour and a cancer is about 3 and 10 times larger than that of the corresponding healthy tissue, respectively. Similar proportions are found for the conductivity.

The application of a proper inversion method to the electromagnetic data may result in quantitative imaging, which could give evidence of the state of breast tissue. The Contrast Source Inversion (CSI) method [6] was specifically chosen for this work. In addition to microwave tomography [4], CSI has been applied, for instance, to magnetic resonance-based electric properties tomography [6], [7], [8]. The combination of microwave and ultrasound imaging by means of CSI has also been investigated [9].

Generally, the microwave tomography system has the same configuration in both transmission and reception [6]. Alternatively, it is possible to have an antenna configuration in which the transmitting and the receiving antennas operate in different positions. Such a device allows adapting the configuration in terms of positions of the receiving and transmitting antennas [10].

This paper presents a parametric analysis of the CSI method applied to a two-dimensional model problem, in which a set of plane waves at 5 GHz impinges on a cylindrical phantom. The parameters under analysis are the dielectric properties and the size of an inclusion within the phantom, that should be detected by the imaging method. In the methods section the description of the model was deepened, and in the chapter of the results the outcomes were described; finally, in the discussion and conclusion parts the pros and cons of the use of the CSI method in this context were summarized.

II. Methods

The CSI method for microwave tomography was implemented in MATLAB 2023a. The configuration of transmitters and receivers used for the tomography is presented in Figure 1. More specifically, 40 receiving antennas were distributed around the phantom, at 7 cm from

the system centre, at 9° from each other. Regarding the incident fields generated by the transmitting antennas, they were obtained by simulating ten pairs of plane waves, propagating towards the phantom centre. This type of transmitting arrangement was selected in accordance with the microwave system described in [10], where this arrangement was used to remove artefacts from the produced qualitative images, employing the subtraction between data obtained from close transmitting directions [10].The simulations were conducted at a single operation frequency of 5 GHz for a two-dimensional case.

A cylindrical phantom with radius of 6 cm was positioned at the centre of the antennas' circular distribution, containing a homogenous material with EPs that approximate the ones of a dense breast [11] (relative electrical permittivity equal to 20 and conductivity equal to 2 S/m). The computational domain was discretized into 150 × 150 pixels with steps of 1 mm. The electromagnetic problem was solved with the method of moments.

The CSI method is an optimization problem where a cost functional is minimized. Two variables, called the contrast source and the contrast, were iteratively reconstructed according to a two-step non-linear conjugate gradient method with Polak-Ribière directions. Assuming to know the geometry of the scatterer, a constraint can be added to the contrast update. Precisely, after each iterative step, a null contrast value was assigned to all the pixels in the external air region. This constraint helps the minimization of the cost at each step and the convergence of the method.

The iterative procedure was stopped after a given number of iterations chosen *a priori*.

CSI provides the contrast map from which the values of the EPs were deduced pixel by pixel [6], [7], [8]. Inputs of the method are the incident electric fields in the phantom location and the total electric field data computed in the receiving antennas' locations. To test the presented CSI algorithm, additive Gaussian noise (2 %) was introduced in the input total electric fields.

To test preliminarily the possible CSI performances in breast lesion detection, a parametric analysis was carried out. It consisted in two phases. First, the effect of different choices of the initial guess in the homogeneous phantom reconstruction were assessed. Then, a circular compartment was included in the phantom and the capability of CSI to detect its presence when varying its contrast with respect to the phantom background, its dimension and its position were investigated.

III. RESULTS

Results are presented here in terms of expected maps of EPs, reconstructed maps of EPs, and plots of expected and reconstructed EPs along the vertical line passing for the system centre. All the results were obtained after 10,000 iterations of CSI.

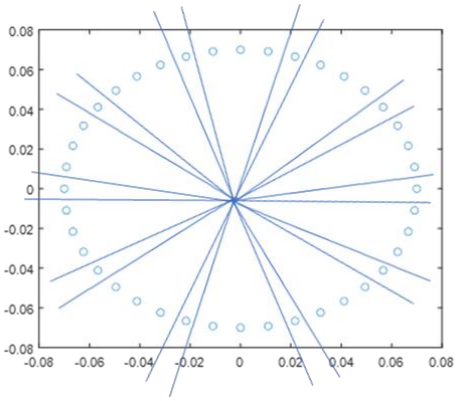

Fig. 1. Configuration of transmitters and receivers chosen for the application of CSI. The lines represent the 20 directions along which the plane waves propagate (converging towards the centre of the phantom). The points represent the 40 receivers, located around the phantom, which collect the data.

The results obtained for the homogenous phantom are reported in Fig. 2 with different choices of the initial guess. At first, conductivity and relative permittivity values of the initial guess were set equal to 1.8 S/m and 19, respectively. Then, they were set equal to 1.5 S/m and 15, and 2.5 S/m and 25, respectively.

In Fig. 3, all the results of the phantom with inclusion are presented. The parametric analysis consisted in eight cases, obtained by combining the three parameters that characterize the inclusion, each one with two possible values. Each case was denoted by the label rRvVpP, where R, V and P are binary digits identifying the radius, the value of the EPs, and the position, respectively. The inclusion radius can be equal to 4 mm (R=0) or 7.5 mm (R=1). The two sets of EP values, representative of increasing contrasts, are: conductivity and relative permittivity of 2.5 S/m and 25 (V=0), respectively, or 4 S/m and 40 (V=1), respectively. Finally, the considered positions are a central one (P=0, centre of the inclusion at 8 mm from the system centre) and a peripheral position (P=1, centre of the inclusion at 30 mm from the system centre). Regarding the EP values of the inclusion, the first case represents a borderline case in which the contrast between the inclusion and the background is low. They could be those of a benign tumour compared to those of the surrounding healthy tissue in a dense breast situation [12]. Table 1 and table 2 show the values of mean and standard deviation of the electrical conductivity and relative permittivity of the inclusion in the reconstructed maps.

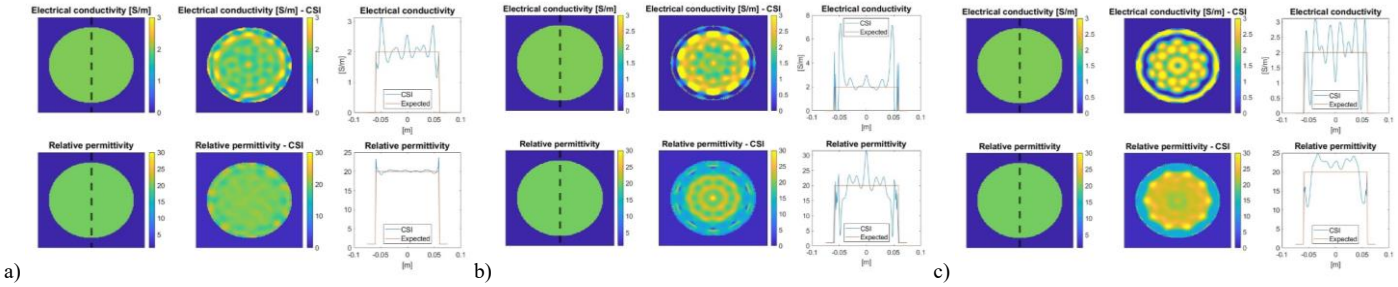

a) b) c)

Fig. 2. Results in case of homogenous phantom using three different initial guesses: σ =1.8 S/m and ε_r=19 (a), σ=1.5 S/m and ε_r=15 (b), and σ=2.5 S/m and ε_r=25 (c). Ground truth (first column), conductivity and relative permittivity reconstructions (second column), histogram of values on a central diameter (third column).

Electrical conductivity		***p0***	***p1***
v0	***r0***	2.14 ± 0.2	2.24 ± 0.28
	r1	2.2 ± 0.27	2.17 ± 0.25
v1	***r0***	2.65 ± 0.35	2.89 ± 0.82
	r1	2.86 ± 0.65	2.89 ± 0.72

Table 1. Inclusion's electrical conductivity (S/m)

Relative permittivity		***p0***	***p1***
v0	***r0***	22.44 ± 0.69	22.42 ± 0.97
	r1	23.07 ± 0.91	22.97 ± 0.94
v1	***r0***	27.55 ± 2.69	27.48 ± 3.53
	r1	29.64 ± 3.56	29.2 ± 3.51

Table 2. Inclusion's relative permittivity

IV. DISCUSSION

The first phase of the analysis was about the effect of the initial guess. The first case, presented in Fig. 2a, shows the reconstruction with an initial guess very close to the expected results. Noise is greater in the conductivity rather than in the relative permittivity, this may be motivated by the ratio $\sigma/(\omega\varepsilon)$ that is lower than 1 at the considered frequency. Despite Gaussian noise was added to the input data, the predominant contribution of the observed noise is structured, which is due to a systematic error introduced by the CSI method. As shown in Fig. 2b and Fig. 2c, if the iterative procedure of CSI was started far from the expected EP values, the reconstructed EPs maps were very different from the expected homogeneous result. Possibly, the iterative procedure got stuck in a local minimum of the cost functional. This finding suggests that a *priori* information is fundamental to build a reasonable initial guess. Alternatively, prior insensitive techniques can be adopted to solve the imaging problem [13] at the cost of an increased complexity of the numerical method.

This observation was considered for the subsequent phase of the analysis, in which a homogeneous contrast was used as initial guess, with conductivity and relative permittivity corresponding to 1.8 S/m and 19, respectively, close to the expected phantom background values. The analysis with the inclusion leads to the following noteworthy results.

Despite the initial guess does not involve indications about the inclusion, the method does not seem to suffer issues related to local minima, suggesting that a good estimation of the background is enough as an initial guess for lesion detection.

The inclusion is visible and detectable in the permittivity maps independently of the considered dimension. In particular, one peak of relative permittivity was reconstructed in the centre of the inclusion when its radius was equal to 4 mm, whereas a ring of large permittivity values appeared at the inclusion periphery when the radius was equal to 7.5 mm, resulting in a couple of peaks in the plot along the phantom diameter. This suggests that the inner part of larger inclusions is more difficult to reconstruct.

The position of the inclusion does not affect the result. In the conductivity maps, the inclusion near the edge was confused with the large systematic errors observed also in the reconstruction of the homogeneous phantom.

Regarding the EP values of the inclusion, the results suggest that the anomaly can be detected even in a borderline case with a low contrast between background and inclusion (V=0). When the contrast is larger (V=1), it becomes more difficult to reach the expected relative permittivity of the inclusion, although a large peak value was obtained. Increasing the number of iterative steps could improve the accuracy of this reconstruction.

V. CONCLUSION

The presented results suggest the importance of the initial guess in the EP reconstruction. In particular, the initial guess on the contrast should not be too far from the sample background, to avoid issues related to local minima in the detection of lesions. This finding can be translated in future clinical practice by assessing preliminary the background properties depending on the patient's breast density, which is known to greatly affect the breast EPs [11].

Because of the different EP values of healthy and pathological breast tissues [5], the obtained results underpin the feasibility of a quantitative non-ionizing mammography using microwave imaging. According to [14], a minimal invasive breast carcinoma has dimension <1cm; a detailed analysis will be performed to identify the minimum inclusion dimension which allows detection.

At the present stage (i.e., a virtual experiment), planewaves in open space are used to simulate the excitations. In future extensions of the present analysis, interactions between the transmitting and receiving antennas as well as the scatterer will be considered, approaching the real imaging system.

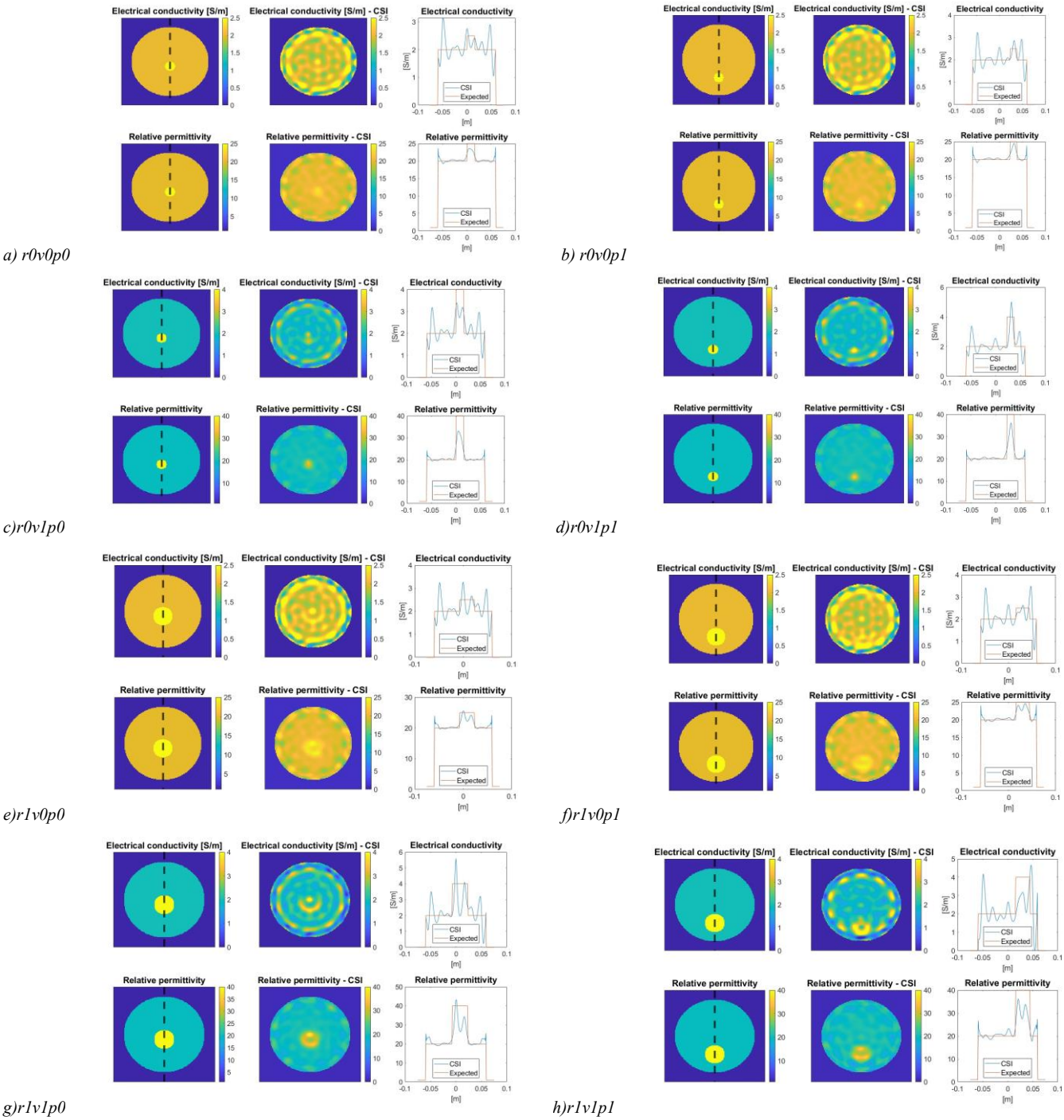

a) r0v0p0 *b) r0v0p1*

c)r0v1p0 *d)r0v1p1*

e)r1v0p0 *f)r1v0p1*

g)r1v1p0 *h)r1v1p1*

Fig. 3 Results varying dimension, positions, and properties of the inclusion. Ground truth (first column), conductivity and relative permittivity reconstructions (second column), histogram of values on a central diameter (third column).

Forthcoming work will be done on the implementation of a system that allows the integration of the results at different frequencies, as in a range of 4-6 GHz, with a fine sampling, with the aim of improving the outcome quality. Moreover, some post-processing strategies could be developed to elaborate the outcomes of CSI and remove the systematic errors found in the background reconstruction, especially in the conductivity maps.

VI. REFERENCES

[1] Á. Yago Ruiz, M. Cavagnaro, and L. Crocco, "An Effective Framework for Deep-Learning-Enhanced Quantitative Microwave

Imaging and Its Potential for Medical Applications", Sensors, vol. 23, no. 2, pp. 643, Jan. 2023.
[2] M. Arnold, E. Morgan, H. Rumgay, A. Mafra, D. Singh, M. Laversanne, J. Vignat, J. R. Gralow, F. Cardoso, S. Siesling, and I. Soerjomataram, "Current and future burden of breast cancer: Global statistics for 2020 and 2040", 2022, Breast (Edinburgh, Scotland), vol. 66, pp. 15–23.
[3] A. Vispa, L. Sani, M. Paoli, A. Bigotti, G. Raspa, N. Ghavami, S. Caschera, M. Ghavami, M. Duranti, and G. Tiberi, "UWB device for breast microwave imaging: phantom and clinical validations", Measurement, vol. 146, pp. 582-589, 2019.
[4] A. Zakaria, C. Gilmor, and J. LoVetri, "Finite-element contrast source inversion method for microwave imaging", Inverse problem, vol. 26, no. 11, Sept. 2010.
[5] Y. Cheng and M. Fu, "Dielectric properties for non-invasive detection of normal, benign, and malignant breast tissues using microwave theories", Thoracic cancer, 9(4), pp. 459–465, 2021.
[6] P. Van den Berg and A. Abubakar, "Contrast Source Inversion Method: State of Art", vol. 34, pp. 189-218, 2001.
[7] R. L. Leijsen, W. M. Brink, Cornelis A. T. van den Berg, A. G. Webb, and R. F. Remis, "3-D Contrast Source Inversion-Electrical Properties Tomography", IEEE Transactions on Medical Imaging, vol. 37, no. 9, pp. 2080-2089, Sept. 2018.
[8] A. Arduino, L. Zilberti, M. Chiampi and O. Bottauscio, "CSI-EPT in Presence of RF-Shield for MR-Coils", IEEE Transactions on Medical Imaging, vol. 36, no. 7, pp. 1396-1404, July 2017.
[9] Y. Qin, T. Rodet, M. Lambert and D. Lesselier, "Joint Inversion of Electromagnetic and Acoustic Data with Edge-Preserving Regularization for Breast Imaging", IEEE Transactions on Computational Imaging, vol. 7, pp. 349-360, 2021.
[10] L. Sani, A. Vispa, R. Loretoni, M. Duranti, N. Ghavami, D. Alvarez Sánchez-Bayuela, S. Caschera, M. Paoli, A. Bigotti, M. Badia, M. Scorsipa, G. Raspa, M. Ghavami, and G. Tiberi, "Breast lesion detection through MammoWave device: Empirical detection capability assessment of microwave images' parameters", PloS one, vol. 16, no. 4, 2021.
[11] J. D. Shea, P. Kosmas, S. C. Hagness, and B. D. Van Veen, "Three-dimensional microwave imaging of realistic numerical breast phantoms via a multiple-frequency inverse scattering technique", Medical physics, vol. 37, no. 8, pp. 4210–4226, 2010.
[12] E. Zastrow, S. K. Davis, M. Lazebnik, F. Kelcz, B. D. V. Veen and S. C. Hagness, "Development of Anatomically Realistic Numerical Breast Phantoms with Accurate Dielectric Properties for Modeling Microwave Interactions with the Human Breast", IEEE Transactions on Biomedical Engineering, vol. 55, no. 12, pp. 2792-2800, Dec. 2008.
[13] Paul M. Meaney and Keith D. Paulsen, "Theoretical Premises and Contemporary Optimizations of Microwave Tomography", Recent Microwave Technologies. IntechOpen, 2022.
[14] P. Querzoli, G. Albonico, S. Ferretti, R. Rinaldi, D. Beccati, S. Corcione, M. Indelli and I. Nenci, "Modulation of biomarkers in minimal breast carcinoma: a model for human breast carcinoma progression" Cancer, vol. 83, no. 1, pp. 89–97, 1998.